

Reactions of Secondary Silanes with $[\{\text{Pr}^i_2\text{PCH}_2\text{CH}_2\text{PPr}^i_2\}\text{Rh}]_2(\mu\text{-H})_2$. A Series of Dinuclear Silyl–Hydride Complexes and Their Possible Involvement in the Catalytic Hydrosilylation of Olefins

Michael D. Fryzuk,^{*,1a} Lisa Rosenberg, and Steven J. Rettig^{1b}

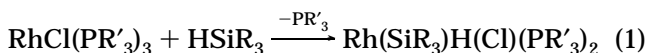
Department of Chemistry, University of British Columbia, 2036 Main Mall,
Vancouver, British Columbia, V6T 1Z1

Received June 13, 1995[®]

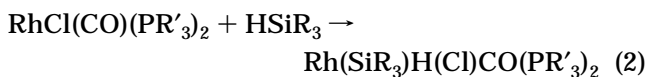
Addition of a 1 equiv of a secondary silane ($\text{RR}'\text{SiH}_2$) to $[(\text{dippe})\text{Rh}]_2(\mu\text{-H})_2$ (**1**) gives the complexes $[(\text{dippe})\text{Rh}]_2(\mu\text{-H})(\mu\text{-}\eta^2\text{-HSiRR}')$ (**2a**, $\text{R} = \text{R}' = \text{Ph}$; **2b**, $\text{R} = \text{R}' = \text{Me}$; **2c**, $\text{R} = \text{Ph}$, $\text{R}' = \text{Me}$; dippe = 1,2-bis(diisopropylphosphino)ethane). X-ray diffraction studies of **2a,b** confirm the presence of a three-center, two-electron, $\text{Rh}\text{--H}\text{--Si}$ bond. The observed fluxionality of **2a–c** in solution is due to exchange of the silicon and rhodium hydrides. Complexes **2a–c** lose hydrogen in the presence of 1 equiv of carbon monoxide to give complexes **3a–c**, $[(\text{dippe})\text{Rh}]_2(\mu\text{-SiRR}')(\mu\text{-CO})$. A catalytic cycle is proposed for the hydrosilylation of olefins by diphenylsilane to give Ph_2SiR_2 ($\text{R} = \text{Et}$) or Ph_2SiHR ($\text{R} = \text{Bu}$), which occurs in the presence of **1**. One of the active species is thought to be $[(\text{dippe})\text{Rh}]_2(\mu\text{-H})(\mu\text{-}\eta^2\text{-HSiPh}_2)$ (**2a**).

Introduction

Most studies of the reactivity of silanes toward rhodium complexes have arisen from investigation of their activity as hydrosilylation catalysts. In particular, Wilkinson's catalyst, $\text{RhCl}(\text{PPh}_3)_3$, has received much attention as a catalyst precursor for the hydrosilylation of various unsaturated organic molecules,² and thus it is not too surprising that the vast majority of known rhodium silyl complexes are derived from this complex and its analogues. As shown in eq 1, five-coordinate

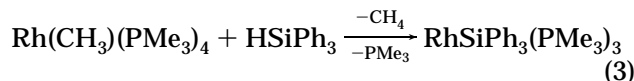


silyl–hydride complexes of Rh(III) can be obtained by oxidative addition of tertiary silanes to $\text{RhCl}(\text{PR}_3)_3$; a wide variety of substituents on silicon can be tolerated, and different phosphine ligands have been examined as well.^{3–7} Octahedral Rh(III) silyl–hydride complexes result upon oxidative addition of tertiary silanes to the related chloro–carbonyl complex $\text{RhCl}(\text{CO})(\text{PR}_3)_2$, as shown in eq 2.³ When a Rh(I) complex contains a

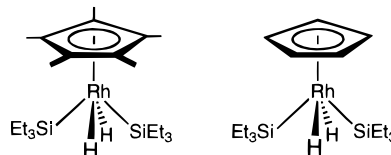


hydrocarbyl ligand, then oxidative addition can be

accompanied by reductive elimination to regenerate a Rh(I) silyl species; an example is shown in eq 3.^{8,9} This

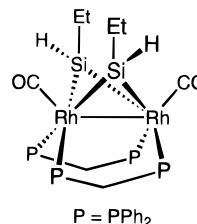


is one of the few known Rh(I) silyl derivatives. Also, reaction of silanes with some “half-sandwich” cyclopentadienyl–rhodium complexes have produced silyl complexes



with rhodium in the rare +5 oxidation state.^{10,11}

There are not many examples in the literature of dinuclear rhodium silyl complexes. In fact, addition of silanes to dinuclear rhodium complexes such as $\text{Rh}_2(\text{PF}_3)_8$ and $[(\text{C}_8\text{H}_{12})\text{RhCl}]_2$ ($\text{C}_8\text{H}_{12} = 1,5\text{-cyclooctadiene}$) typically generates mononuclear products.^{12,13} Studies of the dinuclear rhodium complex $\text{Rh}_2(\mu\text{-H})_2(\text{CO})_2(\mu\text{-dppm})_2$, however, have yielded dinuclear silyl complexes, including that shown (dppm = bis(diphenylphosphino)methane):¹⁴



(8) Thorn, D. L.; Harlow, R. L. *Inorg. Chem.* **1990**, 29, 2017.

(9) Hofmann, P.; Meier, C.; Hiller, W.; Heckel, M.; Reide, J.; Schmidt, M. U. *J. Organomet. Chem.* **1995**, 490, 51.

[®] Abstract published in *Advance ACS Abstracts*, June 1, 1996.
(1) (a) Tel: (604) 822-2897. FAX: (604) 822-2847. E-mail: fryzuk@chem.ubc.ca. (b) Experimental Officer: UBC Crystallographic Service.

(2) Ojima, I. In *The Chemistry of Organic Silicon Compounds*; Patai, S., Rappoport, Z., Eds.; Wiley: New York, 1989; p 1479.

(3) de Charenteney, F.; Osborn, J. A.; Wilkinson, G. *J. Chem. Soc. A* **1968**, 787.

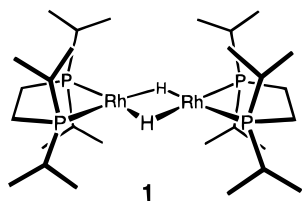
(4) Haszeldine, R. N.; Parish, R. V.; Parry, D. J. *J. Chem. Soc. A* **1969**, 683.

(5) Glockling, F.; Hill, G. C. *J. Chem. Soc. A* **1971**, 2137.

(6) Ojima, I.; Nihonyanagi, M. *J. Chem. Soc., Chem. Commun.* **1972**, 938.

(7) Haszeldine, R. N.; Parish, R. V.; Taylor, R. J. *J. Chem. Soc., Dalton Trans.* **1974**, 2311.

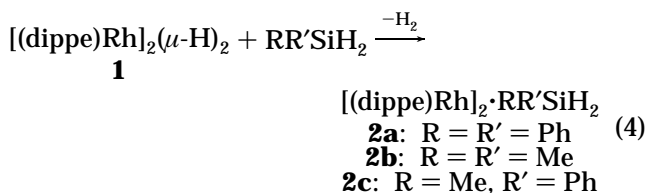
In this work the reactions of a variety of secondary silanes ($RR'SiH_2$) with the dinuclear rhodium hydride complex $[(dippe)Rh]_2(\mu-H)_2$ (**1**; dippe = 1,2-bis(diisopro-



pylphosphino)ethane) are presented, and the characterization and reactivity of the ensuing complexes are discussed. The use of **1** as a catalyst precursor for the hydrosilylation of olefins by diphenylsilane is also described. A possible hydrosilylation catalytic cycle is proposed.

Results and Discussion

Synthesis and Properties of Dinuclear Silyl-Hydride Complexes. We have already reported¹⁵ that the dinuclear rhodium hydride complex $[(dippe)Rh]_2(\mu-H)_2$ (**1**) reacts rapidly with 1 equiv of diphenylsilane (Ph_2SiH_2) to afford a dinuclear product of empirical formula $[(dippe)Rh]_2 \cdot Ph_2SiH_2$ (**2a**) in good yield, with concurrent evolution of 1 equiv of dihydrogen. This reaction may be extended to dimethylsilane (Me_2SiH_2) and methylphenylsilane ($MePhSiH_2$), generating the analogous complexes **2b,c**. Isolated yields of these



complexes vary from 60 to 85% depending on the scale used, due to their high solubility in organic solvents. The complexes are air- and moisture-sensitive both in solution and in the solid state; they are thermally stable in solution, as judged by the fact that heating to 80 °C in *d*₈-toluene in a sealed NMR tube for several days caused no decomposition, as determined by $^{31}P\{^1H\}$ NMR spectroscopy. Labeling studies using the corresponding dideuteride $[(dippe)Rh]_2(\mu-D)_2$ (*d*₂-**1**) show that the oxidative addition of the Si-H bond of Ph_2SiH_2 and reductive elimination of H_2 occurs nonselectively (with complete scrambling of H/D) via a highly fluxional intermediate.

The room-temperature 1H and $^{31}P\{^1H\}$ NMR spectra of complexes **2a-c** suggest highly symmetric structures in solution, where all four phosphorus centers are chemically and magnetically equivalent, as are both rhodium centers. A single rhodium hydride resonance, a sharp multiplet with a relative intensity of 2, is observed in each 1H NMR spectrum. Symmetric doublet

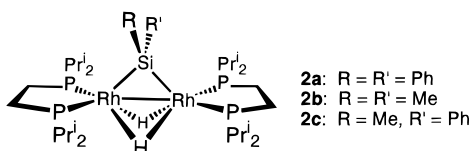


Figure 1. Possible averaged structure in solution for complexes **2a-c**.

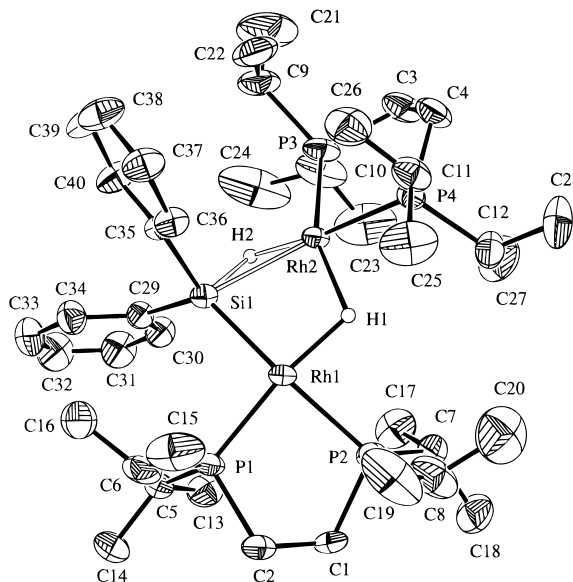


Figure 2. Molecular structure and numbering scheme for $[(dippe)Rh]_2(\mu-H)(\mu-\eta^2-HSiPh_2)$ (**2a**).

or doublet-of-multiplet patterns are observed in the $^{31}P\{^1H\}$ NMR spectra (coupling to ^{103}Rh , $I = 1/2$, 100% natural abundance). These results are consistent with the proposed structure shown in Figure 1, with two bridging hydrides and one bridging silylene ligand. However, the broadness of the doublets observed in the $^{31}P\{^1H\}$ NMR spectra of **2a** and **2c** suggest that these compounds are fluxional; variable-temperature $^{31}P\{^1H\}$ and 1H NMR spectroscopic studies have confirmed that some fluxional process is occurring in which the two hydrides exchange between inequivalent sites. Indeed, a fluxional process must also be occurring to exchange the methyl and phenyl substituents on silicon for **2c**, to give an average structure in solution with four equivalent phosphines. This is discussed in more detail later.

Solid-State Structures of $[(dippe)Rh]_2(\mu-H)(\mu-\eta^2-HSiR_2)$ ($R = Ph$, **2a; $R = Me$, **2b**).** The solid-state structure of the dinuclear complex $[(dippe)Rh]_2(\mu-H)(\mu-\eta^2-HSiPh_2)$ (**2a**) was evident from a single-crystal X-ray diffraction analysis and has already been reported;¹⁵ the analogous structure of $[(dippe)Rh]_2(\mu-H)(\mu-\eta^2-H-SiMe_2)$ (**2b**) was also determined. Both solid-state structures are different from the solution structures proposed in the previous section. ORTEP diagrams of the dinuclear complexes are shown in Figures 2 and 3, and selected bond distances and bond angles for the two structures are shown in Tables 2 and 3. In these structures the two hydride ligands were both located and refined.

The most interesting feature of these two structures is that while one hydride ligand bridges the two Rh centers, the other is found bridging a Rh-Si bond. The average lengthening of the bridged Rh-Si bond relative to the unbridged bond in the two molecules is 0.17 Å, which is consistent with the presence of the bridging

(10) Fernandez, M.; Bailey, P. M.; Bentz, P. O.; Ricci, J. S.; Koetzle, T. F.; Maitlis, P. M. *J. Am. Chem. Soc.* **1984**, *106*, 5458.

(11) Duckett, S. B.; Perutz, R. N. *J. Chem. Soc., Chem. Commun.* **1991**, 28.

(12) Bennett, M. A.; Patmore, D. J. *Inorg. Chem.* **1971**, *10*, 2387.

(13) Aylett, B. J. *J. Organomet. Chem.* **1980**, *9*, 327.

(14) Wang, W.; Eisenberg, R. *J. Am. Chem. Soc.* **1990**, *112*, 1833.

(15) Fryzuk, M. D.; Rosenberg, L.; Rettig, S. J. *Organometallics* **1991**, *10*, 2537.

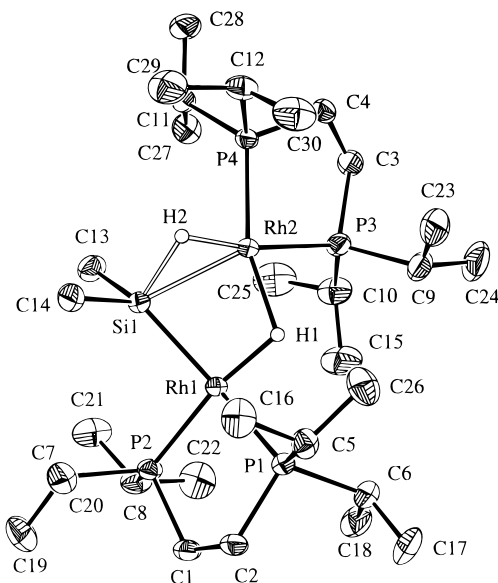


Figure 3. Molecular structure and numbering scheme for $[(\text{dippe})\text{Rh}]_2(\mu\text{-H})(\mu\text{-}\eta^2\text{-HSiMe}_2)$ (**2b**).

Table 1. Crystallographic Data^a

compd	$[(\text{dippe})\text{Rh}]_2(\mu\text{-H})(\mu\text{-HSiPh}_2)$ (2a)	$[(\text{dippe})\text{Rh}]_2(\mu\text{-H})(\mu\text{-HSiMe}_2)$ (2b)
formula	$\text{C}_{40}\text{H}_{76}\text{P}_4\text{Rh}_2\text{Si}$	$\text{C}_{30}\text{H}_{72}\text{P}_4\text{Rh}_2\text{Si}$
fw	914.83	760.69
color, habit	red-orange, irregular	orange, needle
cryst size, mm	$0.20 \times 0.35 \times 0.50$	$0.08 \times 0.15 \times 0.45$
cryst syst	monoclinic	monoclinic
space group	$P2_1/n$	$P2_1/n$
<i>a</i> , Å	19.338(8)	13.386(3)
<i>b</i> , Å	11.223(4)	17.067(4)
<i>c</i> , Å	22.934(9)	17.862(4)
β , deg	112.39(3)	102.69(2)
<i>V</i> , Å ³	4602(6)	3981(1)
<i>Z</i>	4	4
<i>T</i> , °C	21	21
<i>D_c</i> , g/cm ³	1.320	1.319
<i>F</i> (000)	1920	1664
$\mu(\text{Mo K}\alpha)$, cm ⁻¹	8.93	10.21
transmissn factors (rel)	0.91–1.00	0.90–1.00
scan type	$\omega-2\theta$	$\omega-2\theta$
scan range, deg in ω	$1.31 + 0.35 \tan \theta$	$0.89 + 0.35 \tan \theta$
scan speed, deg/min	32 (up to 8 rescans)	16 (up to 8 rescans)
data collected	$+h, +k, \pm l$	$+h, +k, \pm l$
$2\theta_{\text{max}}$, deg	55	60
cryst decay, %	negligible	2.7
total no. of rflns	11 434	12 412
no. of unique rflns	11 112	11 943
<i>R_{merge}</i>	0.036	0.036
no. with $I \geq 3\sigma(I)$	5752	6473
no. of variables	432	342
<i>R</i>	0.037	0.029
<i>R_w</i>	0.043	0.027
GOF	1.46	1.35
max Δ/σ (final cycle)	0.03	0.19 (H coordinate)
residual density, e/Å ³	-0.52, 0.78 (near Rh)	-0.33, 0.37

^a Conditions and definitions: Rigaku AFC6S diffractometer, takeoff angle 6.0°, aperture 6.0×6.0 mm at a distance of 285 mm from the crystal, stationary background counts at each end of the scan (scan/background time ratio 2:1), Mo K α radiation ($\lambda = 0.71069$ Å), graphite monochromator, $\sigma^2(F^2) = [S^2(C + 4B) + (pF^2)^2]/Lp^2$ (*S* = scan speed, *C* = scan count, *B* = normalized background count, $p = 0.03$ for **2a** and 0.01 for **2b**), function minimized $\sum w(|F_o| - |F_c|)^2$, where $w = 4F_o^2/\sigma^2(F_o^2)$, $R = \sum ||F_o| - |F_c||/\sum |F_o|$, $R_w = (\sum w(|F_o| - |F_c|)^2/\sum w|F_o|^2)^{1/2}$, and GOF = $[\sum w(|F_o| - |F_c|)^2/(m - n)]^{1/2}$. Values given for *R*, *R_w*, and GOF are based on those reflections with $I \geq 3\sigma(I)$.

hydride. The Si–H distances are only roughly 0.2 Å longer than a typical Si–H bond length in free silane

Table 2. Selected Bond Lengths (Å) with Estimated Standard Deviations in Parentheses

[(dippe)Rh] ₂ (μ-H)(μ-HSiPh ₂) (2a)			
Rh(1)–Rh(2)	2.937(1)	Rh(2)–Si	2.487(2)
Rh(1)–P(1)	2.213(2)	Rh(2)–H(1)	1.90(6)
Rh(1)–P(2)	2.295(2)	Rh(2)–H(2)	1.61(6)
Rh(1)–Si	2.298(2)	Si–C(29)	1.907(5)
Rh(1)–H(1)	1.71(6)	Si–C(35)	1.902(5)
Rh(2)–P(3)	2.221(2)	Si–H(2)	1.66(6)
Rh(2)–P(4)	2.233(2)		
[(dippe)Rh] ₂ (μ-H)(μ-HSiMe ₂) (2b)			
Rh(1)–Rh(2)	2.8835(6)	Rh(2)–Si(1)	2.463(1)
Rh(1)–P(1)	2.2738(9)	Rh(2)–H(1)	1.91(3)
Rh(1)–P(2)	2.2154(9)	Rh(2)–H(2)	1.51(4)
Rh(1)–Si(1)	2.308(1)	Si(1)–C(13)	1.899(4)
Rh(1)–H(1)	1.65(3)	Si(1)–C(14)	1.899(4)
Rh(2)–P(3)	2.246(1)	Si(1)–H(2)	1.73(4)
Rh(2)–P(4)	2.2165(9)		

Table 3. Selected Bond Angles (deg) with Estimated Standard Deviations in Parentheses

[(dippe)Rh] ₂ (μ-H)(μ-HSiPh ₂) (2a)			
P(1)–Rh(1)–P(2)	87.02(6)	P(4)–Rh(2)–H(2)	172(2)
P(1)–Rh(1)–Si	97.33(6)	H(1)–Rh(2)–H(1)	111(3)
P(1)–Rh(1)–H(1)	170(2)	Rh(1)–Si–C(29)	124.1(2)
P(2)–Rh(1)–Si	164.73(5)	Rh(1)–Si–C(35)	123.5(2)
P(2)–Rh(1)–H(1)	84(2)	Rh(1)–Si–H(2)	101(2)
Si–Rh(1)–H(1)	92(2)	C(29)–Si–C(35)	104.0(2)
P(3)–Rh(2)–P(4)	86.60(6)	C(29)–Si–H(2)	90(2)
P(3)–Rh(2)–H(1)	157(2)	C(35)–Si–H(2)	108(2)
P(3)–Rh(2)–H(2)	85(2)	Rh(1)–H(1)–Rh(2)	109(3)
P(4)–Rh(2)–H(1)	77(2)	Rh(2)–H(2)–Si	99(3)
[(dippe)Rh] ₂ (μ-H)(μ-HSiMe ₂) (2b)			
P(1)–Rh(1)–P(2)	87.45(3)	Si(1)–Rh(2)–H(2)	44(1)
P(1)–Rh(1)–Si(1)	152.36(3)	H(1)–Rh(2)–H(2)	107(2)
P(1)–Rh(1)–H(1)	83(1)	Rh(1)–Si(1)–Rh(2)	74.29(3)
P(2)–Rh(1)–Si(1)	98.12(4)	Rh(1)–Si(1)–C(13)	132.4(1)
P(2)–Rh(1)–H(1)	170(1)	Rh(1)–Si(1)–C(14)	117.4(1)
Si(1)–Rh(1)–H(1)	92(1)	Rh(1)–Si(1)–H(2)	102(1)
P(3)–Rh(2)–P(4)	86.71(3)	Rh(2)–Si(1)–C(13)	108.4(1)
P(3)–Rh(2)–Si(1)	140.65(3)	Rh(2)–Si(1)–C(14)	125.3(1)
P(3)–Rh(2)–H(1)	84(1)	Rh(2)–Si(1)–H(2)	37(1)
P(3)–Rh(2)–H(2)	168(1)	C(13)–Si(1)–C(14)	99.8(2)
P(4)–Rh(2)–Si(1)	116.16(3)	C(13)–Si(1)–H(2)	106(1)
P(4)–Rh(2)–H(1)	159(1)	C(14)–Si(1)–H(2)	91(1)
P(4)–Rh(2)–H(2)	82(1)	Rh(1)–H(1)–Rh(2)	108(2)
Si(1)–Rh(2)–H(1)	82(1)	Rh(2)–H(2)–Si(1)	99(2)

(1.48 ± 0.02 Å),¹⁶ and the Rh–H distances of 1.51(4) and 1.61(6) Å are within the normal range for terminal or bridging hydrides on rhodium. Three-center, two-electron bonds such as these are no longer considered rare for Si–H interactions with transition metals.^{16–19} They are commonly viewed as coordinated Si–H σ -bonds^{16,20–22}—essentially arrested oxidative additions—and are referred to as “agostic” Si–H bonds, a term originally coined to describe the coordination of a C–H σ -bond from an already coordinated ligand to the metal center.²³ Comparison of the relevant bond lengths in the structures of **2a,b** with those for other dinuclear complexes with agostic Si–H bridges suggests that the oxidative addition of the Si–H bond to rhodium

(16) Schubert, U. *Adv. Organomet. Chem.* **1990**, *30*, 151.

(17) Matarasso-Tchiroukhine, E. *J. Chem. Soc., Chem. Commun.* **1990**, 681.

(18) Carreño, R.; Riera, V.; Ruiz, M. A.; Jeannin, Y.; Philoche-Levisalles, M. *J. Chem. Soc., Chem. Commun.* **1990**, 15.

(19) Suzuki, H.; Takao, T.; Tanaka, M.; Moro-oka, Y. *J. Chem. Soc., Chem. Commun.* **1992**, 476.

(20) Crabtree, R. H.; Hamilton, D. G. *Adv. Organomet. Chem.* **1988**, *28*, 299.

(21) Lichtenberger, D. L.; Rai-Chaudhuri, A. *Inorg. Chem.* **1990**, *29*, 975.

(22) Jessop, P. G.; Morris, R. H. *Coord. Chem. Rev.* **1992**, *121*, 155.

(23) Brookhart, M.; Green, M. L. H. *J. Organomet. Chem.* **1983**, *250*, 395.

in **2a** has been arrested at a relatively early stage, while for **2b** the addition has been arrested at an intermediate stage.¹⁶

The strong *trans* influence of the silyl ligand ($-\text{SiR}_3$) manifests itself in the two structures as a lengthening of the P–Rh distances for those phosphines *trans* to the silicon, relative to the other P–Rh distances in the structures.²⁴ The most noticeable effects of the *trans* influence are in the structure of **2a**, where P(2)–Rh(1) is ~ 0.08 Å longer than P(1)–Rh(1) and P(3)–Rh(2). In the structure of **2b** P(1)–Rh(1) is 0.06 Å longer than P(2)–Rh(1) and P(4)–Rh(2). It could be argued that these effects are simply steric in origin, but in that case one would expect the trend to be reversed. For example, in **2a** one would expect P(1) and P(3) to be pushed away from the phenyl groups on silicon, resulting in longer P(1)–Rh(1) and P(3)–Rh(2) bond lengths. Instead, these are the shortest P–Rh bond lengths.

If the Si–H σ -interaction with rhodium is viewed as a single ligand, the geometry at each of the rhodium centers in complexes **2a,b** is roughly square planar, though the two planes are twisted relative to each other. The dihedral angles between the coordination planes defined by P(1), Rh(1), P(2) and by P(3), Rh(2), P(4) in the two structures are 116.6 and 133.8° for **2a** and **2b**, respectively. This twisting of the chelate rings relative to each other is probably due mainly to the size of the bridging $\eta^2\text{-HSiR}_2$ ligand. The Rh–Rh separations observed in these structures are similar to a range of distances seen for the complexes $[(\text{P}_2)\text{Rh}]_2(\mu\text{-H})(\mu\text{-X})$ (where $\text{P}_2 = \text{dippe}$, $(\text{P}(\text{OMe})_3)_2$; $\text{X} = \eta^2\text{-CR}=\text{CHR}$). For example, in the vinyl hydride complex $[(\text{dippe})\text{Rh}]_2(\mu\text{-H})(\mu\text{-}\eta^2\text{-CH}=\text{CH}_2)$ ²⁵ (**5**), the Rh–Rh distance is 2.8655(5) Å, while for $[(\text{MeO})_3\text{P}]_2\text{Rh}_2(\mu\text{-}\eta^2\text{-C}(\text{Tol}^p)=\text{CH}(\text{Tol}^p)(\mu\text{-H}))$ ²⁶ the separation is 2.936(1) Å.

Variable-Temperature $^{31}\text{P}\{^1\text{H}\}$ and ^1H NMR Spectroscopy of **2a–c.** The variable-temperature $^{31}\text{P}\{^1\text{H}\}$ and ^1H (hydride region) NMR spectra of $[(\text{dippe})\text{Rh}]_2(\mu\text{-H})(\mu\text{-}\eta^2\text{-HSiPh}_2)$ (**2a**) are shown in Figures 4 and 5, respectively. While at room temperature the $^{31}\text{P}\{^1\text{H}\}$ NMR spectrum of **2a** is a slightly broad doublet, at lower temperatures the spectrum becomes more complex, illustrating two dynamic processes, one with a coalescence at about -40 °C and the other with a coalescence at about -80 °C. At -66 °C the $^{31}\text{P}\{^1\text{H}\}$ NMR spectrum indicates a species with two equivalent phosphines and two other, inequivalent phosphines (three doublets of integral ratio 2:1:1), whereas at -96 °C the spectrum shows a broad set of signals attributable to the presence of four inequivalent phosphines; thus, at very low temperatures we observe a spectrum that corresponds with the solid-state structure of **2a**. In the intermediate-temperature regime, the $^{31}\text{P}\{^1\text{H}\}$ NMR spectrum is consistent with structure **B** in Scheme 1. The presence of a single hydride resonance for both the Si–H and the Rh–H moieties in the room-temperature ^1H NMR spectrum suggests that the fluxionality in **2a** also involves exchange of the bridging hydride H_b and the silicon “hydride” H_a . A possible mechanism for this

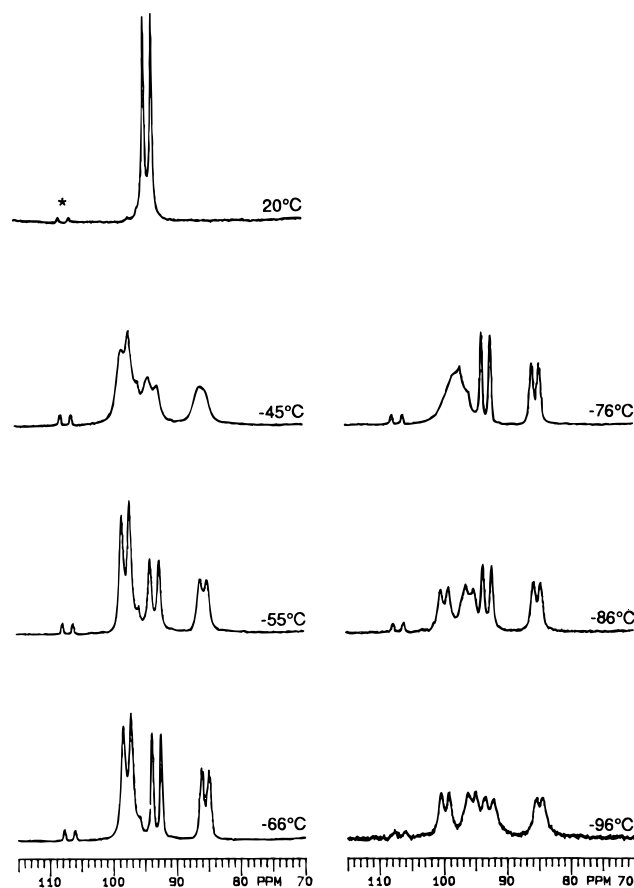


Figure 4. Variable-temperature 121.4 MHz $^{31}\text{P}\{^1\text{H}\}$ NMR spectra of $[(\text{dippe})\text{Rh}]_2(\mu\text{-H})(\mu\text{-}\eta^2\text{-HSiPh}_2)$ (**2a**) in C_7D_8 (a small amount of **1** is indicated by an asterisk).

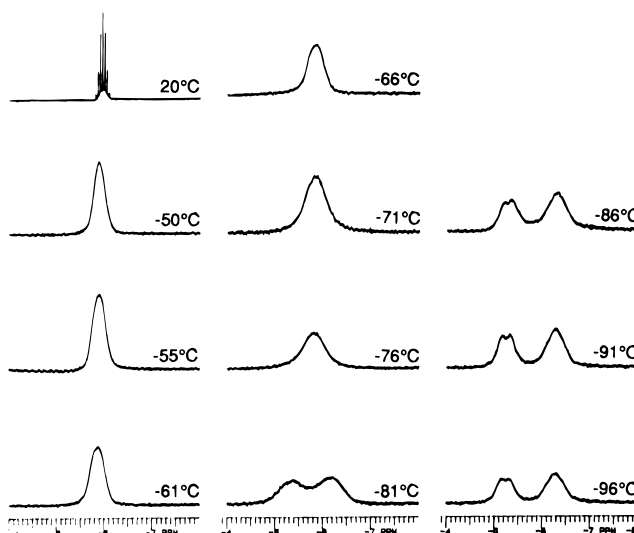


Figure 5. Variable-temperature 300 MHz ^1H NMR spectra (hydride region) of $[(\text{dippe})\text{Rh}]_2(\mu\text{-H})(\mu\text{-}\eta^2\text{-HSiPh}_2)$ (**2a**) in C_7D_8 .

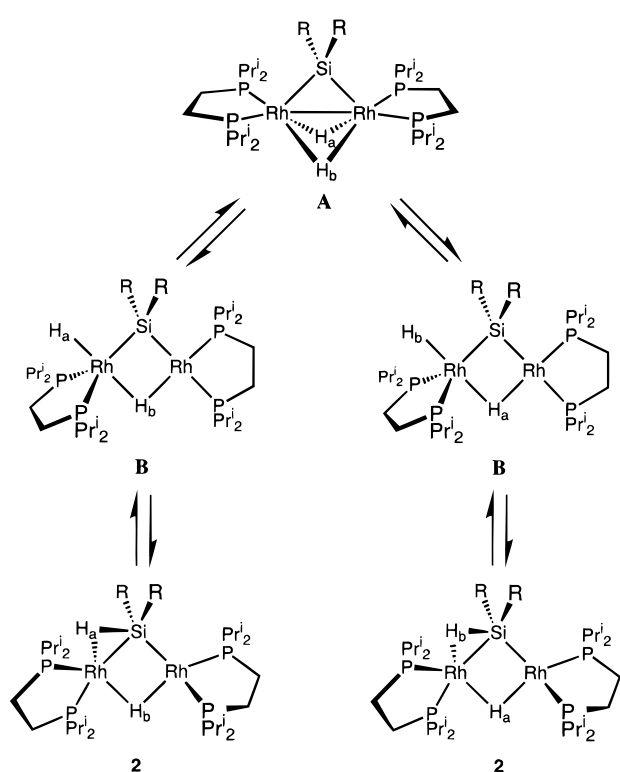
exchange is shown in Scheme 1; starting at the bottom left, the complete oxidative addition of the Si– H_a bond of **2** gives the species **B**, with a bridging silylene fragment and a terminal hydride. The changes in geometry at the rhodium centers required to accommodate this correspond to the lower temperature process observed in the $^{31}\text{P}\{^1\text{H}\}$ NMR spectra. The terminal hydride subsequently swings into a bridging position, yielding a symmetric intermediate with the structure **A** (proposed structure **2a** in Figure 1). The reverse of

(24) Collman, J. P.; Hegedus, L. S.; Norton, J. R.; Finke, R. G. *Principles and Applications of Organotransition Metal Chemistry*; University Science Books: Mill Valley, CA, 1987.

(25) Fryzuk, M. D.; Jones, T.; Einstein, F. W. B. *Organometallics* **1984**, *3*, 185.

(26) Burch, R. R.; Shusterman, A. J.; Muetterties, E. L.; Teller, R. G.; Williams, J. M. *J. Am. Chem. Soc.* **1983**, *105*, 3546.

Scheme 1



these steps, with H_b swinging out to the terminal position instead of H_a , accounts for the exchange the two hydrides.¹⁵

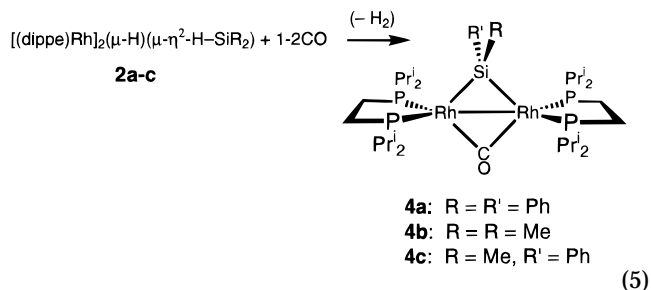
The variable-temperature 1H NMR spectra shown in Figure 5 are also consistent with the hydride fluxionality described: at -91 to -96 °C the spectrum shows two distinct hydride signals at -5.28 and -6.26 ppm. This decoalescence corresponds to the higher temperature process observed in the $^{31}P\{^1H\}$ NMR spectra (i.e., the exchange involving structures **A** and **B** in Scheme 1). An approximate J_{H-P} value of 40 Hz observed for the lower field signal (-5.28 ppm) is larger than the usual *cis* H-P coupling but smaller than most *trans* coupling constants measured in similar compounds. Because of the broadening due to coupling to phosphorus and rhodium no ^{29}Si satellites are seen for either of these hydride signals.²⁷ It seems reasonable to conclude that the three-center, two-electron Rh-H-Si bond observed in the solid-state structure of **2a** does exist in solution but is labile with respect to complete oxidative addition of the Si-H bond to the Rh center, rendering the silyl hydride complex fluxional. A ΔG^\ddagger (193 K) value of 8.6 ± 0.2 kcal/mol was calculated for **2a** for the fluxional process exchanging structures **A** and **B** in Scheme 1, using the coalescence of the hydride signals in the 1H NMR spectra.

For the methylphenylsilyl analogue **2c**, $[(dippe)Rh]_2(\mu-H)(\mu-\eta^2-HSiMePh)$, the activation barrier for exchange of the hydrides must be lower than for the diphenyl derivative, since a decoalescence for the hydride signals was not achieved even at -84 °C. As shown in Figure 6, at that temperature the $^{31}P\{^1H\}$ NMR spectrum of **2c** shows three signals: a broad

doublet at 97.8 ppm, a doublet at 92.8 ppm, and a broad singlet at 87.2 ppm, in a 2:1:1 ratio. A similar spectrum (three doublets of integral ratio 2:1:1) is observed for **2a** at -55 °C, with almost identical chemical shift separations between the analogous peaks (Figure 4). The 1H and $^{31}P\{^1H\}$ NMR spectra of $[(dippe)Rh]_2(\mu-H)(\mu-\eta^2-HSiMe_2)$ (**2b**) show even less change at low temperature than those for the methylphenylsilyl analogue. For **2b** there is only a slight broadening of the doublet observed in the $^{31}P\{^1H\}$ NMR spectrum and of the hydride signal at -6.3 ppm in the 1H NMR spectrum at -85 °C. Given that all three complexes **2a-c** show resonances in their room-temperature $^{31}P\{^1H\}$ NMR spectra with practically identical chemical shifts, and given the similar shifts observed in the low-temperature $^{31}P\{^1H\}$ NMR spectra of **2a** and **2c**, it is likely that the low-temperature limit for the $^{31}P\{^1H\}$ spectra of all three complexes would show peaks with similar shifts. Thus, the differences in coalescence temperatures for **2a-c** result mainly from differences in the activation barrier to hydride exchange. There is a steady reduction of this activation barrier to exchange in complexes **2a-c** which corresponds to the stepwise replacement of phenyl groups with methyl groups; $\Delta G^\ddagger_{2a} > \Delta G^\ddagger_{2c} > \Delta G^\ddagger_{2b}$ for the process.

One further point concerns the methylphenylsilyl-hydride complex $[(dippe)Rh]_2(\mu-H)(\mu-\eta^2-HSiMePh)$ (**2c**). The above exchange mechanism in effect for these molecules in solution (Scheme 1) does not explain why the room-temperature $^{31}P\{^1H\}$ NMR spectrum for this complex indicates the presence of four equivalent phosphines despite the unsymmetrically substituted silicon in the averaged structure. This result requires the substituents on silicon to be exchanging very rapidly, which may be due to the coordinated Si-H bond rapidly dissociating from and reassociating with the metal center, as shown in Scheme 2. Rotation around the remaining Rh-Si bond and inversion at the Si center via a transition state labeled **C** would complete the exchange. This process must be occurring for all three silyl hydride complexes **2a-c**.

Displacement of Hydrogen by Carbon Monoxide in the Silyl Hydride Complexes 2a-c. Dinuclear rhodium complexes with bridging carbonyl and silylene units (**3a-c**) are generated by the addition of approximately 1 equiv of CO to the silyl hydrides **2a-c** (eq 5). Complex **3a** has been isolated in pure form, and



complexes **3b,c** have been observed in solution, though they were not isolated pure in the solid state. Addition of an excess of CO to the silyl hydride complexes gives a mixture of products other than **3a-c** which are difficult to separate from each other and which have not been identified. The approximately 1:1 reactions of the silyl hydrides with CO are of interest because they

(27) ^{29}Si NMR spectra for **2a** and **2b** show signals that are too broad and poorly resolved to give any information on the connectivity at silicon in these complexes, even at low temperature (for **2a**). This is probably due to the extensive coupling of silicon to other spins, combined with the fluxionality of the complexes.

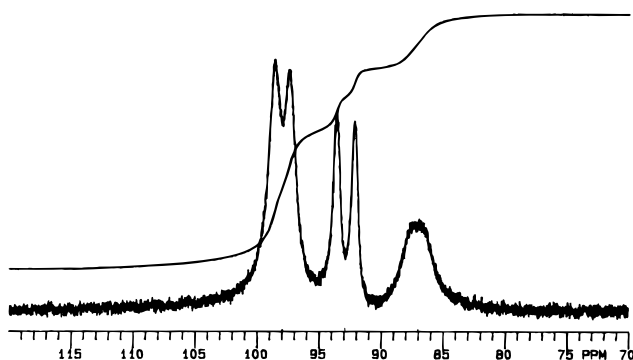
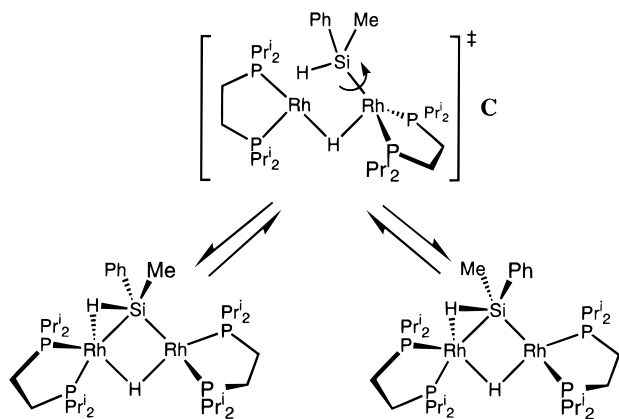


Figure 6. Low-temperature 121.4 MHz $^{31}\text{P}\{^1\text{H}\}$ NMR spectrum of $[(\text{dippe})\text{Rh}]_2(\mu\text{-H})(\mu\text{-}\eta^2\text{-HSiMePh}_2)$ (**2c**) in C_7D_8 at -84°C .

Scheme 2



demonstrate the ease with which hydrogen is removed from the Rh_2Si core. The complete oxidative addition of the second Si–H bond of diphenylsilane to Rh is facile, as is the subsequent elimination of H_2 .

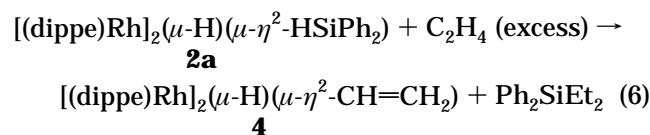
The $^{31}\text{P}\{^1\text{H}\}$ NMR spectra of complexes **3a–c** show simple doublets of multiplets, indicating that in solution all four phosphines are chemically equivalent. A structure which is consistent with the NMR data contains tetrahedral rhodium centers. For the unsymmetrically substituted μ -methylphenylsilylene complex **3c**, the simple $^{31}\text{P}\{^1\text{H}\}$ NMR spectrum observed must be due to fluxionality of the complexes in solution. One possibility is through the formation of fully planar, dinuclear structures which rapidly equilibrate with the proposed tetrahedral ground-state geometry.

Catalytic Hydrosilylation of Ethylene and 1-Butene. The complex $[(\text{dippe})\text{Rh}]_2(\mu\text{-H})_2$ (**1**) has been shown to be an efficient catalyst precursor for the hydrogenation of olefins at ambient temperature and pressure. For example, its use as a catalyst precursor for the hydrogenation of 1-hexene (with a substrate/catalyst ratio of approximately 1700) gives turnover numbers in the range $850\text{--}950\text{ h}^{-1}$.²⁸ Given the reactivity of this complex toward both hydrogen and olefins, one of the initial goals of this study was to confirm that **1** is also a catalyst precursor for the hydrosilylation of olefins.

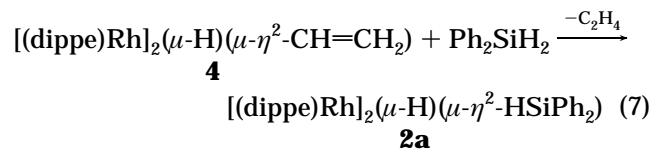
The complex $[(\text{dippe})\text{Rh}]_2(\mu\text{-H})_2$ (**1**) was found to be a catalyst precursor for the hydrosilylation of both ethylene and 1-butene by diphenylsilane. The product of

hydrosilylation of ethylene is the double-addition product diethyldiphenylsilane, Ph_2SiEt_2 . None of the single-addition product, ethyldiphenylsilane, was observed in reaction mixtures, even before completion (i.e., disappearance of diphenylsilane). When this catalytic reaction was monitored by ^1H NMR, a turnover number of 960 h^{-1} was calculated. The hydrosilylation of 1-butene results in the formation of the single-addition compound *n*-butyldiphenylsilane, $(n\text{-Bu})\text{SiHPh}_2$, the expected anti-Markovnikov addition product.²⁹

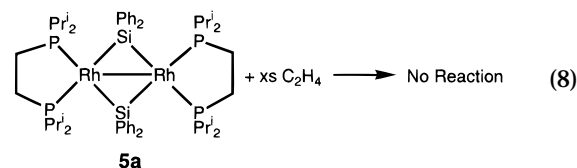
A number of stoichiometric reactions relevant to the hydrosilylation of ethylene catalyzed by **1** were carried out in order to determine if the active species in the catalytic cycle could be identified. For example, when ethylene is added to the starting dihydride dimer $[(\text{dippe})\text{Rh}]_2(\mu\text{-H})_2$ (**1**), the dinuclear vinyl hydride complex $[(\text{dippe})\text{Rh}]_2(\mu\text{-H})(\mu\text{-}\eta^2\text{-CH=CH}_2)$ (**4**) is formed.²⁵ When ethylene is added to $[(\text{dippe})\text{Rh}]_2(\mu\text{-H})(\mu\text{-}\eta^2\text{-HSiPh}_2)$ (**2a**), the same vinyl hydride complex **4** is isolated, along with diethyldiphenylsilane (eq 6). How-



ever, when diphenylsilane is added to the vinyl hydride complex **4**, the silyl hydride complex **2a** is regenerated. No diethyldiphenylsilane is observed in the ^1H NMR spectrum of this reaction, shown in eq 7; it is assumed



that addition of the silane to the vinyl hydride causes elimination of ethylene. The bis(μ -silylene) complex $[(\text{dippe})\text{Rh}]_2(\mu\text{-SiPh}_2)_2$ (**5a**) is certainly present in any mixture of **1** and excess silane.³⁰ However, no reaction is observed between **5a** and ethylene, which rules out the possible participation of the bis(μ -silylene) complex in the hydrosilylation cycle.



The above reactions suggest that the hydrosilylation of ethylene catalyzed by **1** could involve the silyl-hydride **2a** as one of the active species in the catalytic cycle. A possible catalytic cycle for the hydrosilylation of ethylene based on this dinuclear active species is shown in Figure 7. If, in the presence of excess silane, the catalyst is converted to **5a**, this would "shut down" the hydrosilylation. However, with every oxidative addition of Ph_2SiH_2 to **1** to produce **2a**, or to **2a** to produce **5a**, dihydrogen is evolved. In the presence of H_2 , the bis(μ -silylene) complex **5a** is converted back to the silyl-hydride complex **2a**.³⁰ Thus, in the catalytic

(28) Fryzuk, M. D.; Piers, W. E.; Einstein, F. W. B.; Jones, T. *Can. J. Chem.* **1989**, *67*, 883.

(29) Elschenbroich, C.; Salzer, A. *Organometallics: A Concise Introduction*, 2nd ed.; VCH: New York, 1992.

(30) Fryzuk, M. D.; Rosenberg, L.; Rettig, S. J., unpublished results.

99.6 atom % D) and deuterated toluene (C_7D_8 , 99.6 atom % D) were purchased from MSD Isotopes and dried over 4 Å molecular sieves. The dried, deuterated solvents were then degassed using three "freeze–pump–thaw" cycles and were vacuum-transferred before use. Carbon monoxide, ethylene, and 1-butene were purchased from Matheson Gas Products. Deuterium gas was purchased from Matheson and passed through a glass coil immersed in liquid nitrogen to remove any traces of water and oxygen.

1H NMR spectra were recorded on Varian XL-300, Bruker WP-200, Bruker WH-400, or Bruker AMX-500 spectrometers. With d_6 -benzene as solvent the spectra were referenced to C_6D_5H at 7.15 ppm, and with d_8 -toluene as solvent the spectra were referenced to the CD_2H residual proton at 2.09 ppm. $^{31}P\{^1H\}$ NMR spectra were recorded at 121.4 MHz on the Varian XL-300 or at 202.3 MHz on the Bruker AMX-500 and were referenced to external $P(OMe)_3$ at 141.0 ppm relative to 85% H_3PO_4 . $^1H\{^{31}P\}$ NMR spectra were recorded on the Bruker AMX-500. $^2H\{^1H\}$ NMR spectra were run in C_6H_6 at 46.0 MHz on the Varian XL-300 and were referenced to residual solvent deuterons at 7.15 ppm. $^{29}Si\{^1H\}$ and ^{29}Si NMR were run at 59.6 MHz on the Varian XL-300 and were referenced to external TMS at 0.0 ppm.

Elemental analyses were carried out by Mr. P. Borda of this department. Gas chromatography/mass spectrometry was carried out by Ms. L. Madilao of this department.

Literature methods were used to prepare $[(dippe)Rh]_2(\mu-H)_2$ (**1**)^{25,42} $[(dippe)Rh]_2(\mu-D)_2$ (**d₂-1**),²⁵ and $[(dipp)Rh]_2(\mu-H)_2$.⁴² Ph_2SiH_2 and $MePhSiH_2$ were purchased from Aldrich Chemical Co., dried by refluxing over calcium hydride overnight, and distilled. Me_2SiH_2 was prepared by reduction of Me_2SiCl_2 , purchased from Aldrich, using $LiAlH_4$, by a slight modification of the literature procedure.⁴³

Syntheses of Complexes and Reactivity Studies. **$[(dippe)Rh]_2(\mu-H)(\mu-\eta^2-HSiPh_2)$ (**2a**).** To a stirred, dark green solution of $[(dippe)Rh]_2(\mu-H)_2$ (**1**; 150 mg, 0.205 mmol) in toluene (3 mL) was added dropwise a solution of diphenylsilane (38 mg, 0.206 mmol) in toluene (2 mL) to give a dark red solution. The toluene was removed under vacuum, and the residue was dissolved in hexanes. After filtration of the solution through a Celite pad, red crystals were obtained from a minimum volume of hexanes (or pentane) by cooling to $-40^\circ C$. Yield: 77% (145 mg). 1H NMR (C_6D_6 , ppm): H_{ortho} 8.06 (dd, 4H, $^3J_{H_m-H_o} = 7.9$ Hz, $^4J_{H_p-H_o} = 1.4$ Hz); H_{meta} 7.27 (mult, 4H); H_{para} 7.14 (tt, 2H, $^3J_{H_p-H_m} = 6.6$ Hz); $CH(CH_3)_2$ 1.96 (mult, 8H, $^3J_{H-H} = 6.8$ Hz (from $^1H\{^{31}P\}$ NMR)); PCH_2CH_2P 1.25 (d, 8H, $^2J_{P-H} = 13.1$ Hz); $CH(CH_3)_2$ 1.05 (dd, 24H, $^3J_{P-H} = 15.1$ Hz, $^3J_{H-H} = 7.1$ Hz); $CH(CH_3)_2$ 0.95 (dd, 24H, $^3J_{P-H} = 12.2$ Hz, $^3J_{H-H} = 6.9$ Hz); $Rh-H$ -6.17 (sept, 2H, $J_{Rh-H} = 14$ Hz = J_{P-H}). $^{31}P\{^1H\}$ NMR (C_6D_6 , ppm): 94.0 (br d, $^1J_{Rh-P} = 155$ Hz). ^{29}Si NMR (C_7D_8 , ppm): 137–141 (br mult, at room temperature), 129–143 (br mult, at $-89^\circ C$). Anal. Calcd for $C_{40}H_{76}P_4Rh_2Si$: C, 52.52; H, 8.37. Found: C, 52.32; H, 8.45.

$[(dippe)Rh]_2(\mu-H)(\mu-\eta^2-HSiMe_2)$ (2b**).** One equivalent of dimethylsilane (0.139 mmol, 103 mmHg in a 25.2 mL constant volume bulb) was vacuum-transferred to a dark green solution of $[(dippe)Rh]_2(\mu-H)_2$ (**1**; 102 mg, 0.139 mmol) in frozen toluene (8 mL) at $-196^\circ C$. The solution was warmed to room temperature, by which time the solution had changed to a deep red color. The toluene was removed under vacuum, and the residue was dissolved in hexanes. After filtration of the solution through a Celite pad, red crystals were obtained from a minimum volume of hexanes (or pentane) by cooling to $-40^\circ C$. Yield: 85% (93 mg). 1H NMR (C_6D_6 , ppm): $CH(CH_3)_2$ 2.05 (overlapping d sept, 8H); PCH_2CH_2P 1.33 (d, 8H, $^2J_{P-H} = 12.9$ Hz); $CH(CH_3)_2$ 1.23 (dd, 24H, $^3J_{P-H} = 15.0$ Hz, $^3J_{H-H} = 7.2$ Hz); $Si(CH_3)_2$ 1.12 (s, 6H); $CH(CH_3)_2$ 1.03 (dd, 24H, $^3J_{P-H} =$

12.3 Hz, $^3J_{H-H} = 6.9$ Hz); $Rh-H$ -6.25 (mult, 2H). Note: for **2b** in d_8 -toluene the $Si(CH_3)_2$ resonance is seen at 1.02 ppm, a solvent-related, upfield shift of 0.10 ppm. $^{31}P\{^1H\}$ NMR (C_6D_6 , ppm): 94.2 (d mult, $J_{Rh-P} = 159$ Hz). ^{29}Si NMR (C_7D_8 , ppm): 163 (mult). Anal. Calcd for $C_{30}H_{72}P_4Rh_2Si$: C, 45.57; H, 9.18. Found: C, 45.70; H, 9.23.

$[(dippe)Rh]_2(\mu-H)(\mu-\eta^2-HSiMePh)$ (2c**).** This complex was prepared by the same method as for **2a** (210 mg, 0.287 mmol of **1**; 35 mg, 0.286 mmol of $MePhSiH_2$). Dark, reddish brown crystals were obtained in 62% yield (151 mg). 1H NMR (C_6D_6 , ppm): H_{ortho} 8.00 (d, 2H, $^3J_{H_m-H_o} = 6.6$ Hz); H_{meta} 7.29 (t, 2H, $^3J_{H_p-H_m-H_o-H_m}$ (av) = 7.3 Hz); H_{para} 7.15 (mult, 1H); $CH(CH_3)_2$ 1.97 (mult, 8H); PCH_2CH_2P , $SiCH_3$ 1.28–1.36 (overlapping d and s, 11H); $CH(CH_3)_2$ 1.20 (dd, 12H, $^3J_{P-H} = 14.8$ Hz, $^3J_{H-H} = 7.0$ Hz); $CH(CH_3)_2$ 1.12–0.94 (mult, 36H); $Rh-H$ -6.00 (pt, 2H, $J_{P-H} = 19.5$ Hz, $J_{Rh-H} = 15.1$ Hz). $^{31}P\{^1H\}$ NMR (C_6D_6 , ppm): 94.3 (d mult, $^1J_{Rh-P} = 160$ Hz). Anal. Calcd for $C_{35}H_{74}P_4Rh_2Si$: C, 49.30; H, 8.75. Found: C, 49.62; H, 8.86.

$[(dipp)Rh]_2(\mu-H)(\mu-\eta^2-HSiPh_2)$ (2d**).** This complex was prepared by the same method as for **2a** (96 mg, 0.13 mmol of $[(dipp)Rh]_2(\mu-H)_2$; 22 mg, 0.12 mmol of Ph_2SiH_2). Dark, reddish brown crystals were obtained in 64% yield (72 mg). 1H NMR (C_7D_8 , ppm): H_{ortho} 8.12 (d, 4H, $^3J_{H_m-H_o} = 7.8$ Hz); H_{meta} 7.23 (t, 4H); H_{para} 7.15 (t, 2H, $^3J_{H_m-H_p} = 6.3$ Hz); $PCH_2CH_2CH_2P$, $CH(CH_3)_2$ 1.90–1.60 (overlapping mult, 12H); $PCH_2CH_2CH_2P$ 1.18 (br mult, 8H); $CH(CH_3)_2$ 1.09 (dd, 24H, $^3J_{H-P} = 14.4$ Hz, $^3J_{H-H} = 7.2$ Hz); $CH(CH_3)_2$ 0.99 (dd, 24H, $^3J_{H-P} = 11.8$ Hz, $^3J_{H-H} = 6.4$ Hz); $Rh-H$ -8.55 (pt, 2H, $J_{P-H} = 20.9$ Hz, $J_{Rh-H} = 14.6$ Hz). $^{31}P\{^1H\}$ NMR (C_7D_8 , ppm): 37.2 (d, $^1J_{Rh-P} = 155$ Hz). Anal. Calcd for $C_{42}H_{80}P_4Rh_2Si$: C, 53.50; H, 8.55. Found: C, 53.16; H, 8.71.

$[(dippe)Rh]_2(\mu-D)(\mu-\eta^2-DSiPh_2)$ (d₂-2a**).** A solution of $[(dippe)Rh]_2(\mu-SiPh_2)_2$ (**5a**;³⁰ 75 mg, 0.068 mmol) in 10 mL of toluene in a thick-walled reactor bomb was degassed by two freeze–pump–thaw cycles and then cooled to $-196^\circ C$. Deuterium gas was introduced to 1 atm pressure, and the reactor bomb was sealed. The mixture was warmed to room temperature, giving a D_2 pressure of 4 atm. The solution was stirred at room temperature for 12–16 h, during which time the bright orange changed to a deep red color. A workup procedure identical with that described for **2a** was followed, giving red crystals in 64% yield (40 mg). In the 1H NMR spectrum of the product the signal due to the bridging hydrides was absent. 2H NMR (C_6H_6 , ppm): -5.92 (br s, $w_{1/2} = 14$ Hz).

Reaction of $[(dippe)Rh]_2(\mu-D)_2$ with Ph_2SiH_2 . A procedure identical with that described for the preparation of $[(dippe)Rh]_2(\mu-H)(\mu-\eta^2-HSiPh_2)$ (**2a**) was followed using **d₂-1** (61 mg, 0.083 mmol). 1H and 2H NMR spectroscopy suggested a product mixture of d_0 -, d_1 -, and d_2 -**2a**, by comparison with spectra of authentic d_0 -**2a** and d_2 -**2a** complexes.

$[(dippe)Rh]_2(\mu-SiPh_2)(\mu-CO)$ (4a**).** To a red solution of $[(dippe)Rh]_2(\mu-H)(\mu-\eta^2-HSiPh_2)$ (**2a**; 85 mg, 0.092 mmol) in toluene (3 mL) in a thick-walled reactor bomb was added approximately 2 equiv of carbon monoxide (0.184 mmol, 136 mmHg in a 25.2 mL bulb) by vacuum transfer. After the solution was warmed to room temperature, the toluene was removed under vacuum. The rust-brown residues were reprecipitated from a minimum volume of hexanes at $-40^\circ C$; a brown powder was obtained. Yield: 70% (61 mg). 1H NMR (C_6D_6 , ppm): H_{ortho} 8.29 (d, 4H, $^3J_{H_m-H_o} = 7.5$ Hz); H_{meta} 7.30 (t, 4H); H_{para} 7.15 (mult, 2H); $CH(CH_3)_2$ 2.11 (br s, 8H); PCH_2CH_2P 1.35 (d, 8H, $^2J_{P-H} = 13.2$ Hz); $CH(CH_3)_2$ 1.07 (dd, 24H, $^3J_{P-H} = 14.7$ Hz, $^3J_{H-H} = 6.9$ Hz); $CH(CH_3)_2$ 0.90 (dd, 24H, $^3J_{P-H} = 11.5$ Hz, $^3J_{H-H} = 7.1$ Hz). $^{31}P\{^1H\}$ NMR (C_6D_6 , ppm): 79.8 (d mult, $^1J_{Rh-P} = 161$ Hz). IR (KBr pellet): ν_{CO} 1703.4 cm^{-1} (s). Anal. Calcd for $C_{41}H_{74}OP_4Rh_2Si$: C, 52.34; H, 7.93. Found: C, 52.21; H, 8.07.

$[(dippe)Rh]_2(\mu-SiMe_2)(\mu-CO)$ (4b**).** This complex was prepared using the same method as for **4a** and has been identified in solution using NMR spectroscopy, but it was not isolated in a pure form. 1H NMR (C_6D_6 , ppm): $CH(CH_3)_2$ 2.14

(42) Fryzuk, M. D.; McConville, D. H.; Rettig, S. J. *J. Organomet. Chem.* **1993**, 445, 245.

(43) Doyle, M. P.; DeBruyn, D. J.; Donnelly, S. J.; Kooistra, D. A.; Odubela, A. A.; West, C. T.; Zonnebelt, S. M. *J. Org. Chem.* **1974**, 39, 2740.

(mult, 8H); $\text{PCH}_2\text{CH}_2\text{P}$ 1.40 (d, 8H, $^2J_{\text{P-H}} = 13.2$ Hz); $\text{Si}(\text{CH}_3)_2$ 1.28 (s, 6H); $\text{CH}(\text{CH}_3)_2$ 1.15 (dd, 24H, $^3J_{\text{P-H}} = 15.1$ Hz, $^3J_{\text{H-H}} = 7.0$ Hz); $\text{CH}(\text{CH}_3)_2$ 1.04 (dd, 24H, $^3J_{\text{P-H}} = 11.8$ Hz, $^3J_{\text{H-H}} = 7.1$ Hz). $^{31}\text{P}\{^1\text{H}\}$ NMR (C_6D_6 , ppm): 82.9 (br d, $^1J_{\text{Rh-P}} = 172$ Hz).

[(dippe)Rh] $_{\text{2}}$ (μ -SiMePh)(μ -CO) (4c). This complex was prepared using the same method as for **4a** and has been identified in solution using NMR spectroscopy, but it was not isolated in a pure form. ^1H NMR (C_6D_6 , ppm): H_{ortho} 7.94 (d, 2H, $^3J_{\text{Hm-Ho}} = 6.0$ Hz); H_{meta} 7.33 (t, 2H); H_{para} 7.15 (t, 1H, $^3J_{\text{Hm-Hp}} = 7.5$ Hz); $\text{CH}(\text{CH}_3)_2$ 2.23 (mult, 8H); $\text{PCH}_2\text{CH}_2\text{P}$ 1.70 (s, 4H); $\text{PCH}_2\text{CH}_2\text{P}$, SiCH_3 , $\text{CH}(\text{CH}_3)_2$ 1.58–1.17 (overlapping mult, 19H); $\text{CH}(\text{CH}_3)_2$ 1.03 (mult, 36H). $^{31}\text{P}\{^1\text{H}\}$ NMR (C_6D_6 , ppm): 81.6 (br d mult, $^1J_{\text{Rh-P}} = 172$ Hz).

Reaction of [(dippe)Rh] $_{\text{2}}$ (μ -H)(μ - η^2 -HSiPh $_2$) with C_2H_4 . A dark red solution of [(dippe)Rh] $_{\text{2}}$ (μ -H)(μ - η^2 -HSiPh $_2$) (**2a**; 25 mg, 0.027 mmol) in d_8 -toluene (0.6 mL) was placed in a sealable NMR tube. The tube was attached to a vacuum line by a needle valve adapter, and slightly less than 1 atm of ethylene was introduced. The tube was cooled to -196°C and then sealed. After 1 week the solution color had changed to a lighter orange, and ^1H and $^{31}\text{P}\{^1\text{H}\}$ NMR spectra showed the presence of [(dippe)Rh] $_{\text{2}}$ (μ -H)(μ - η^2 -CH=CH $_2$) (**4**),²⁵ dissolved ethylene (^1H NMR (ppm, C_7D_8) 5.4 (s)), and some compound containing the SiPh $_2$ fragment, as determined by the presence of signals in the aromatic region of the ^1H NMR spectrum.

The sealed NMR tube was cut open, and the solvent and excess ethylene were removed from the sample *in vacuo*. The residues were dissolved in hexanes and passed down a small column of alumina to remove the vinyl hydride complex **4**. A ^1H NMR spectrum of the eluted compound showed it to be diethyldiphenylsilane, by comparison with an authentic sample prepared by the addition of excess EtMgBr to dichlorodiphenylsilane. ^1H NMR (C_6D_6 , ppm): H_{ortho} 7.62–7.53 (mult, 4H); H_{meta} , H_{para} 7.38–7.16 (mult, 6H); CH_2CH_3 1.18–0.88 (mult, 10H). $^{13}\text{C}\{^1\text{H}\}$ NMR (CDCl_3 , ppm relative to CDCl_3 at 77.0): C_{ipso} 136.26; C_{meta} 134.97; C_{ortho} , C_{para} 129.10, 127.80; C_{methyl} 7.47; $\text{C}_{\text{methylene}}$ 3.96. A HETCOR (^{13}C , ^1H) experiment carried out on the Bruker AMX-500 machine shows the alkyl resonances in the ^1H NMR spectrum to be as follows (ppm): CH_2CH_3 1.004 (q, 4H, $^3J_{\text{H-H}} = 8$ Hz); CH_2CH_3 0.982 (t, 6H). Mass spec (EI; m/e): 240 (M^+), 211, 183, 159, 131, 105, 79.

Reaction of [(dippe)Rh] $_{\text{2}}$ (μ - η^2 -CH=CH $_2$) (4**) with 1 Equiv of Ph_2SiH_2 .** To a solution of [(dippe)Rh] $_{\text{2}}$ (μ -H)(μ - η^2 -CH=CH $_2$) (**4**; 24 mg, 0.032 mmol) in toluene (5 mL) was added a solution of 1 equiv of diphenylsilane (6 mg, 0.032 mmol) in toluene (3 mL). The originally pale orange solution immediately darkened to a deep red-orange color. The solvent was removed *in vacuo*, and the residues were dissolved in d_6 -benzene for analysis by NMR spectroscopy. The only product observed in the $^{31}\text{P}\{^1\text{H}\}$ NMR spectrum was [(dippe)Rh] $_{\text{2}}$ (μ -H)(μ - η^2 -HSiPh $_2$) (**2a**). In the ^1H NMR spectrum the expected resonances due to **2a** were observed. No signals due to Ph_2SiEt_2 were observed.

Catalytic Reactions. Typical Conditions for the Hydrosilylation of Ethylene by Diphenylsilane Using [(dippe)Rh] $_{\text{2}}$ (μ -H) $_2$ (1**) as Catalyst.** A 253 mg (1.38 mmol) amount of diphenylsilane was dissolved in 2.5 mL of toluene, and this solution was placed in a 50 mL reactor bomb with a stirbar. The reactor bomb was attached to the vacuum line, degassed by evacuation of the head space, and then placed under 1 atm of ethylene. The catalyst (**1**; 0.014 mmol, 0.25 mL of a 0.55 M solution in toluene) was added to the substrate solution by syringe under a strong flow of ethylene. The reactor bomb was left open to the manifold full of ethylene, which was kept at 1 atm by periodic addition of more gas from the cylinder. The mixture was stirred for 24 h, at which time it was taken into the glovebox and the catalyst was removed on a Florisil column. The product mixture was analyzed by both GC-MS and ^1H NMR spectroscopy, which showed that all of the diphenylsilane had been consumed. The major product was diethyldiphenylsilane (estimated at >90%).

Mass spectrometric data for diethyldiphenylsilane are listed above in the description of the reaction of ethylene with **2a**, as are the ^1H and $^{13}\text{C}\{^1\text{H}\}$ NMR spectroscopic data.

Progress of the Reaction Monitored by ^1H NMR. Diphenylsilane (126 mg, 0.700 mmol) was dissolved in 3.0 mL of d_6 -benzene, and this solution was placed in a 250 mL reactor bomb with a stirbar. The reactor bomb was attached to the vacuum line, degassed by evacuation of the head space, and then placed under 1 atm of ethylene. This substrate solution was stirred for 15 min before the addition of the catalyst, to ensure saturation of the solution with ethylene. The catalyst (**1**; 0.014 mmol, 10 mg in 1.0 mL of d_6 -benzene) was added by syringe to the substrate solution under a strong flow of ethylene. The reactor bomb was left open to the manifold full of ethylene, which was kept at 1 atm by periodic addition of more gas from the cylinder. Samples of the mixture were withdrawn periodically by syringe, under a strong flow of ethylene. ^1H NMR spectra were run within 10 min of removal of the samples from the mixture, and in some cases $^{31}\text{P}\{^1\text{H}\}$ NMR spectra were run afterwards.

The first sample was withdrawn from the catalytic mixture 3 min after the catalyst was added to the substrate. Its ^1H NMR spectrum showed that 100% conversion of Ph_2SiH_2 to Ph_2SiEt_2 had already occurred. Three more samples removed from the reaction mixture over the next 2 h showed the same ratio of product to starting material. The assumption that the hydrosilylation reaction was finished in 3 min leads to a turnover number of 16 mol min^{-1} (mol of catalyst) $^{-1}$ (or 16 min^{-1} , which is 960 h^{-1}). The $^{31}\text{P}\{^1\text{H}\}$ NMR spectra of the samples all showed [(dippe)Rh] $_{\text{2}}$ (μ -H)(μ - η^2 -HSiPh $_2$) (**2a**) to be the major complex in solution.

Hydrosilylation of 1-Butene by Diphenylsilane Using [(dippe)Rh] $_{\text{2}}$ (μ -H) $_2$ (1**) as Catalyst.** In a glovebox, diphenylsilane (248 mg, 1.35 mmol) was dissolved in 1.5 mL of d_6 -benzene, and this solution was placed in a reactor bomb with a stir bar. The catalyst [(dippe)Rh] $_{\text{2}}$ (μ -H) $_2$ (**1**; 2 mg, 0.003 mmol) was added to the diphenylsilane solution. The dark green solid immediately changed to orange and began to dissolve, and bubbles were evolved. The bomb was attached to a vacuum line, and the head space was evacuated before the bomb and the vacuum manifold were filled with 1 atm of 1-butene. The mixture was stirred for 24 h; then the head space was evacuated and a ^1H NMR spectrum was run.

The initial spectrum showed the reaction had not gone to completion. To remove the volatile starting material, the NMR sample was placed under vacuum while being cooled in an ice bath. ^1H NMR spectroscopy showed the only silicon-containing product to be *n*-butyldiphenylsilane and a very small amount of triphenylsilane (a product of disproportionation of diphenylsilane, which probably formed before the 1-butene was added to the reaction mixture).

For *n*-butyldiphenylsilane: ^1H NMR (C_6D_6 , ppm) H_{ortho} 7.64 (mult, 4H), H_{meta} , H_{para} 7.24 (mult, 6H), Si-H 5.19 (t, 1H, $^3J_{\text{H-H}} = 3.2$ Hz, $^1J_{\text{Si-H}} = 192$ Hz (measured from ^{29}Si satellites)), $\text{SiCH}_2\text{CH}_2\text{CH}_2\text{CH}_3$ 1.54 (mult, 2H), $\text{SiCH}_2\text{CH}_2\text{CH}_2\text{CH}_3$ 1.40 (mult, 2H), $\text{SiCH}_2\text{CH}_2\text{CH}_2\text{CH}_3$ 1.17 (mult, 2H), $\text{SiCH}_2\text{CH}_2\text{CH}_2\text{CH}_3$ 0.88 (t, 3H, $^3J_{\text{H-H}} = 7.3$ Hz); Mass spec (m/e ; EI) 240 (M^+), 183, 162, 134, 105, 84.

Calculation of ΔG^\ddagger for the Hydride Exchange in **2a.** ΔG^\ddagger was calculated using the value for the rate constant k_C (where $k_C = \pi\Delta\nu_C/2^{1/2}$) in the Eyring equation⁴⁴

$$\Delta G^\ddagger = -RT_C \ln[(k_C h)/(k_B T_C)]$$

where R = the gas constant, T_C = temperature of coalescence, $\Delta\nu_C$ = peak separation at the low- T limit, h = Planck constant, and k_B = Boltzmann constant. For the hydride resonances in the variable-temperature ^1H NMR spectra of **2a**, $T_C = 193$ K (-80°C) and $\Delta\nu_C = 309$ Hz. The coalescence temperature was

estimated visually from the spectra and has an error of approximately ± 5 K.

X-ray Crystallography Analyses of [(dippe)Rh]₂(μ -H)-(μ -H-SiR₂) (R = Ph, **2a; R = Me, **2b**).** Crystallographic data appear in Table 1. The final unit-cell parameters were obtained by least squares on the setting angles for 25 reflections with $2\theta = 31.2$ – 44.7° for **2a** and 25.2 – 33.1° for **2b**. The intensities of 3 standard reflections, measured every 200 reflections throughout the data collections, decayed uniformly by 2.7% for **2b** and remained constant for **2a**. The data were processed⁴⁵ and corrected for Lorentz and polarization effects, decay (for **2a**), and absorption (empirical; based on azimuthal scans for three reflections).

The structures were solved by conventional heavy-atom methods. The non-hydrogen atoms of both structures were refined with anisotropic thermal parameters. The metal and silyl hydride atoms were refined with isotropic thermal parameters. All other hydrogen atoms were fixed in idealized positions (staggered methyl groups, C–H = 0.98 Å, $B_H = 1.2B_{\text{bonded atom}}$). Corrections for secondary extinction were not necessary. Neutral atom scattering factors and anomalous

dispersion corrections for all atoms were taken from ref 46. Final atomic coordinates and equivalent isotropic thermal parameters are given in the Supporting Information, and selected bond lengths and angles appear in Tables 2 and 3. Measured and calculated structure factor amplitudes are available from the authors.

Acknowledgment. Financial support for this work was provided by the NSERC (operating grants to M.D.F. and a postgraduate scholarship to L.R.). We also thank Johnson Matthey for the generous loan of RhCl₃·3H₂O.

Supporting Information Available: Complete tables of non-hydrogen atom parameters, bond lengths and angles, calculated hydrogen atom parameters, anisotropic thermal parameters, torsion angles, intermolecular contacts, and least-squares planes for **2a,b** (51 pages). Ordering information is given on any current masthead page.

OM950450D

(45) TEXSAN: Structure Analysis Package (VMS Version 5.1); Molecular Structure Corp., The Woodlands, TX, 1985.

(46) *International Tables for X-Ray Crystallography*; Kynoch Press: Birmingham, U.K. (present distributor Kluwer Academic Publishers: Boston, MA), 1974; Vol. IV, pp 99–102, 149.